

Dynamics of hydrogen, oxygen, and dislocations in yttrium by acoustic spectroscopy

G. Cannelli

Dipartimento di Fisica, Università della Calabria, Arcavacata di Rende (CS) I-87036, Italy

R. Cantelli

Dipartimento di Fisica, Università di Roma "La Sapienza," P.le A. Moro, Roma I-00185, Italy

F. Cordero

CNR, Istituto di Acustica "O.M. Corbino," Via Cassia 1216, Roma I-00189, Italy

F. Trequatrini

Dipartimento di Fisica, Università di Roma "La Sapienza," P.le A. Moro, Roma I-00189, Italy

(Received 19 December 1996)

The nature of the numerous thermally activated processes occurring in yttrium has been investigated by acoustic spectroscopy in polycrystalline samples. The measurements have been carried out between 1.1 and 600 K in the kHz range, varying the concentration of interstitial hydrogen and oxygen in annealed and deformed samples. Four processes have been observed, besides the main dissipation peak around room temperature due to the formation or dissolution of H pairs and that at liquid He temperature attributed to H tunneling. The processes below 300 K have been interpreted in terms of the motion of interstitial hydrogen trapped by oxygen or dragged by dislocations, while the large relaxation detected around 450 K has been attributed to the hopping of oxygen in a solid solution. [S0163-1829(97)00621-8]

I. INTRODUCTION

The hcp rare-earth metals ($R = Y, Sc, Ho, Er, Tm, Lu$) are at present the object of considerable investigative effort for their intriguing properties when they combine with hydrogen. The interest is both of technological and fundamental nature: These metals can absorb massive quantities of hydrogen¹ (e.g., up to $x = 3$ in YH_x) with promising perspectives for hydrogen storage; their hydrides exhibit metal-insulator transitions accompanied by drastic changes in the optical properties;² the high mobility of hydrogen in the hcp lattice allows the observation at low temperature of effects associated with the hopping³⁻¹¹ and tunneling motion of the H atom.^{7,12-15} On the other hand, a thorough characterization of these metals at low impurity content is still lacking¹⁶ because of their strong affinity with O and H; the samples are easily contaminated during high-temperature treatments, but it is difficult to determine the exact contents of O and H. A common method of determining the total amount of impurities in metals is the evaluation of the residual resistivity at 0 K, which is due to the electron scattering by foreign atoms. The values of the ratios between room temperature and the residual resistivity (RRR) reported in the literature for the hcp rare-earth metals are well below 50; for comparison, carefully prepared Nb samples have $RRR \sim 10\,000$.¹⁷

It has been established^{1,18} that in the $R(H/D)_x$ systems hydrogen populates mainly the tetrahedral (T) interstitial sites, with little octahedral (O) occupancy. As the temperature is lowered, hydrogen tends to order in pairs, occupying next-nearest-neighbor T sites along the c axis with a bridging metal atom between the two H atoms; this ordering prevents hydride precipitation so that hydrogen remains in a solid solution down to 0 K even for x as high as 0.2–0.3.

Moreover, the pairs form chains along the c axis with some correlation between chains.

The dynamical properties of the atomic impurities in hcp rare-earth metals have been attributed up to now nearly exclusively to the motion of hydrogen, because most investigations have been concerned with the YH_x and ScH_x alloys at high H concentration. The mobility of H consists of long-range and local motion mechanisms and has been observed on at least three different time scales. Slow motion, characterized by an activation energy of ~ 0.6 eV, has been associated with the long-range diffusion via $T-O-T$ jumps and has been studied by the Gorsky effect,⁴ quasielastic neutron scattering (QNS),¹⁹⁻²¹ and nuclear magnetic resonance (NMR);^{22,23} about the same activation energy and hopping rates have been derived from the anelastic relaxation process observed around room temperature and attributed to H pair formation or dissolution.^{1,6,11} Instead, fast motion of hydrogen is involved in local tunneling between next-nearest-neighbor T sites, as revealed at low temperature by NMR,^{12,13} acoustic spectroscopy,⁷ and ultrasonic attenuation (UA).^{14,15} Finally, rates two orders of magnitude faster than the latter ones have been observed over the same temperature range by QNS.¹⁹⁻²¹ The relation between the two types of local motion remains an aspect which has to be still clarified.

Although the anelasticity of Y has been extensively studied in the last years, only the relaxation process observed around room temperature has been unambiguously interpreted. That process is attributed to a Zener-type mechanism of stress-induced ordering of the H pairs.^{6,11} High-sensitivity acoustic spectroscopy measurements in yttrium have revealed an unexpectedly rich relaxation spectrum,⁷ even in samples which are generally considered pure in the literature. The nature of these processes has not been clarified yet, but their appearance denotes that in yttrium several types of im-

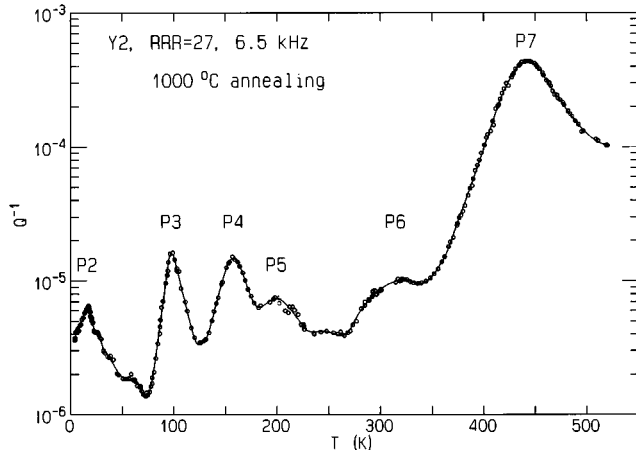


FIG. 1. Anelastic relaxation spectrum of annealed polycrystalline yttrium.

perfections, other than hydrogen, play a role which cannot be ignored for a full understanding of the physical properties of this element and its alloys.

We report a study of the relaxation processes observed in pure polycrystalline yttrium in the temperature range 1.1–600 K. Evidence is given that the detected processes are correlated with the presence of interstitial hydrogen, oxygen, hydrogen-impurity complexes, and dislocations interacting with gaseous impurities.

II. EXPERIMENT

The samples were rectangular bars ($\sim 40 \times 4.4 \times 2 \text{ mm}^3$), cut from different plates of polycrystalline yttrium purchased from the Ames Laboratory, and here labeled as Y0, Y1, Y2, and Y3. The gaseous impurities of the samples Y0 and Y1 were 880 at ppm H, 540 at ppm O, and 60 at ppm N in the “as-received” state, while sample Y2 contained 2700 at ppm O and 300 at ppm N. The impurity content of Y3 was not determined, but was close to that of Y2 since it had a similar history.

The possible variations of the interstitial impurities were monitored between the experiments by the residual resistivity ratio (RRR) measured using a standard dc four-probe technique. The total impurity content deduced from the RRR may be underestimated in the case of impurity clustering or precipitation, since the electron scattering by clustered atoms is lower than that from the same isolated atoms.

In the thermal treatments for H outgassing and for reducing the dislocation density, the samples were wrapped in zirconium foils, with a Mo wire preventing the contact with the foils, and annealed between 1000 and 1250 °C in vacuum in the 10^{-8} mbar range; finally, they were cooled to room temperature in less than 10 min.

The elastic energy dissipation (Q^{-1}) measurements were carried out on both cooling and heating at a rate lower than 1 K/min by electrostatically exciting the samples on different flexural vibration modes in the frequency range 1–33 kHz.

III. RESULTS AND DISCUSSION

Figure 1 presents the acoustic spectroscopy measurement carried out in sample Y2 (RRR=27) between 1.1 and 600 K

TABLE I. Parameters of the anelastic relaxation processes in yttrium.

	τ_0 (s)	E (eV)	ΔE (eV)	α
P3	3×10^{-13}	0.15	<0.01	1
P4	5.8×10^{-13}	0.25	0.05	0.9
P5		0.6		$0.4 \div 0.7$
P6	1×10^{-13}	0.55		
P7	$10^{-12} - 10^{-14}$	0.70	0	0.9

after annealing at 1000 °C. The anelastic relaxation spectrum displays six well-resolved peaks here labeled as P2, P3, P4, P5, P6, and P7 with increasing temperature; one more process manifests itself with a tail (not shown here) appearing below 2 K. This spectrum can be assumed as representative of the anelasticity of yttrium. All the peaks are thermally activated processes and, except P2 (see Ref. 7), follow the Arrhenius law in the temperature range here explored.

The relaxation parameters of the processes (Table I) have been determined by fitting the experimental curves with the expression

$$Q^{-1} = \Delta(T) \frac{1}{(\omega\tau)^\alpha + (\omega\tau)^{-\alpha}}, \quad (1)$$

where ω is the angular vibration frequency, τ the relaxation time following the Arrhenius law, and α is the Fuoss-Kirkwood width parameter;²⁴ $\alpha=1$ for single Debye relaxation, while $\alpha<1$ produces broadened peaks. The relaxation intensity $\Delta(T)$ is proportional to $(\Delta\lambda)^2$, where $\Delta\lambda$ is the change of the local distortion due to the defect jump. In the case of hopping between two nonequivalent sites 1 and 2 with energy separation ΔE , the relaxation intensity, which is also proportional to the product of the respective populations, becomes

$$\Delta(T) \propto \frac{1}{T} \frac{c_1 c_2}{c} \propto c \frac{1}{T} \text{sech}^2\left(\frac{\Delta E}{2k_B T}\right), \quad (2)$$

where c_1 and c_2 are the populations of sites 1 and 2. The site energy difference may be due to the nonequivalence of the sites or to long-range interactions among defects. Equation (2) has a maximum at $k_B T = 0.65 \Delta E$, displays the usual T^{-1} dependence for $k_B T > \Delta E$, and tends to zero at low temperature. Moreover, assuming the Arrhenius law, the relaxation rate becomes

$$\tau^{-1} = \tau_{12}^{-1} + \tau_{21}^{-1} = \tau_0^{-1} e^{-E/k_B T} \cosh\left(\frac{\Delta E}{2k_B T}\right), \quad (3)$$

where E is the mean activation energy for hopping between the two nonequivalent sites.

A. Slow motion of hydrogen

Figure 2 shows the anelastic relaxation spectra measured on heating in sample Y0 in the “as-received state” as cut from a plate (curve 1) and in sample Y1 after the first (1000 °C, curve 2) and third (1250 °C, curve 3) annealing. Five peaks can be clearly resolved in the 1–300 K tempera-

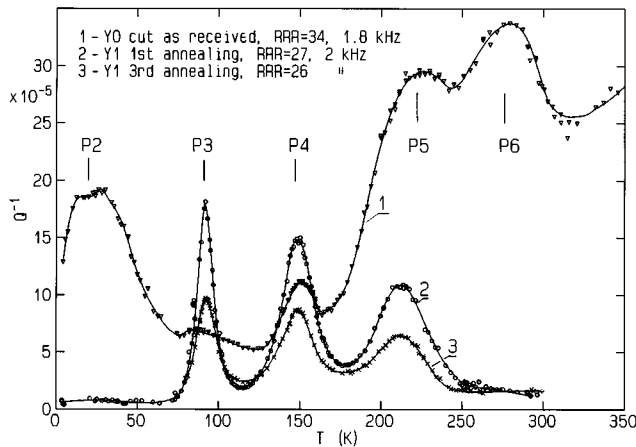


FIG. 2. Anelastic relaxation spectra on heating of sample Y0 in the as-received state (curve 1, RRR=34) and of sample Y1 after the first annealing (1000 °C, curve 2, RRR=27) and third annealing (1250 °C, curve 3, RRR=26).

ture range. It is now accepted that $P2$ is due to H tunneling^{7,14} and $P6$ to the formation or dissolution of H pairs;^{6–11} instead, the nature of the other peaks has not been convincingly clarified yet. Our investigation confirms the relaxation parameters of $P6$ reported in the literature,^{1,6,11} and this process will not be discussed further.

A comparison among the relaxation spectra suggests the following considerations. In sample Y0, where we expect the lowest O content (RRR=34) and an appreciable dislocation density due to cutting, the H tunneling peak $P2$, the H-pair peak $P6$, and peak $P5$ are predominant (curve 1); moreover, the height of $P6$ denotes that the as-received sample contains an amount of interstitial hydrogen which could be of the order of some at. %.⁹ In sample Y1, cut from the same bar, the first annealing (RRR=27, curve 2) suppresses the processes $P2$ and $P6$, both ascribed to hydrogen with certainty, reduces $P5$, and enhances $P3$ and $P4$. The RRR decreased from 52 in the as-received state down to 27, indicating O contamination. After the second and third annealing (RRR=26, curve 3), also $P3$ and $P4$ decrease due the progression of the H outgassing.

Interstitial hydrogen was certainly always present in all the samples; indeed, due to the strong affinity of the rare earths to hydrogen, unwanted quantities of this element can remain in the material even after UHV annealing. Also dislocations are present in the samples: they are produced not only by cutting, but also during the temperature variations; as in other hcp polycrystals, the anisotropic thermal expansion produces plasticity phenomena.²⁵

The following considerations suggest that $P5$ is caused by a mechanism involving dislocations and interstitial hydrogen: (i) The process is more developed in sample Y0 where the dislocation density and the H concentration are higher than in Y1; (ii) the relaxation curve, about twice broader than a single Debye peak (Table I), is not compatible with point-defect relaxation; (iii) a relaxation, with similar features, has been observed in plastically deformed polycrystalline Y.⁸ The mechanism of peak $P5$ should be similar to those reported in transition metals (Nb, Ta, V) and attributed to the relaxation of dislocations dragging interstitial solute

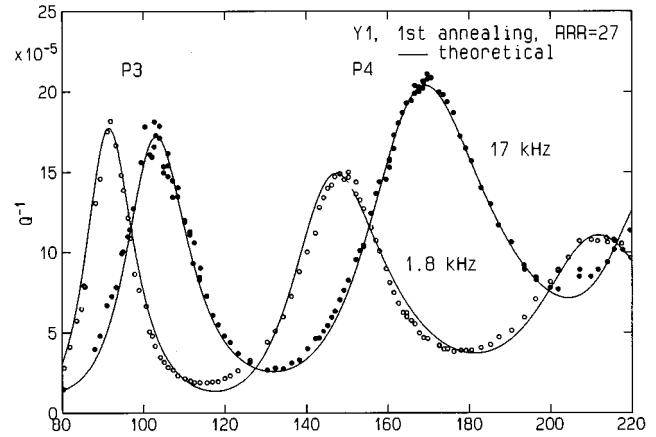


FIG. 3. Best fit to the relaxation curves of $P3$, $P4$, and $P5$ in sample Y1 measured on heating at two vibration frequencies. For details on the fit, see the text and Table I.

impurities,^{26,27} which in the present case are the H interstitial atoms. According to this picture, the observed decrease of $P5$ after annealing can be explained by the concomitant reduction of the dislocation density and H concentration.

Peaks $P3$ and $P4$ are both rather narrow, the Fuoss-Kirkwood parameter being $\alpha \approx 0.9-1$ (Table I). This fact indicates point-defect relaxation, without the involvement of dislocations. Since both O and H are present, the peaks should be due to the local motion of H near the O atoms which are immobile below 300 K; indeed, peaks $P3$ and $P4$ in Fig. 2 are more pronounced in sample Y1, which has a higher O content. We will not propose specific geometries for H hopping, since even the occupaton of interstitial O in Y is not known (presumably it is octahedral); nonetheless, it is possible to extract some information from the peak intensities at different frequencies and impurity concentrations.

Figure 3 shows a fit of $P3$ and $P4$ measured at 1.8 and 17 kHz on heating using Eqs. (1) and (3); the fact that the intensity of $P4$ rises with temperature denotes relaxation between nonequivalent sites with an energy difference $\Delta E \sim 0.05$ eV, as deduced by the fit.

Figures 4(a) and 4(b) present the influence of different H and O charges on the anelastic relaxation spectrum of sample Y1; the curves are numbered in chronological sequence. Curves 1 and 2 are obtained after the first and third annealings, respectively (see Fig. 2). Figure 4(a) displays the effect of 2.5 at. % H charge (curve 3), while Fig. 4(b) shows the evolution with the following charge treatments: Simultaneous H outgassing and 0.5 at. % O charge at 600 °C (curve 4); 0.2 at. % H charge (curve 5); additional 0.2 at. % H charge (curve 6).

The strong hydrogenation suppresses $P3$, $P4$, and $P5$ (curve 3) and at the same time restores $P2$ and $P6$, which are due to the fast and slow motion of hydrogen, respectively. The suppression of $P3$ and $P4$ can be interpreted as a “blocking effect” caused by the saturation of the trap sites around O. Similarly, the suppression of $P5$ can be due to a reduction of the dislocation mobility in a dense atmosphere of H atoms. The effect of this intense H charge explains why the intermediate temperature processes are not detected in the strongly hydrogenated alloys.

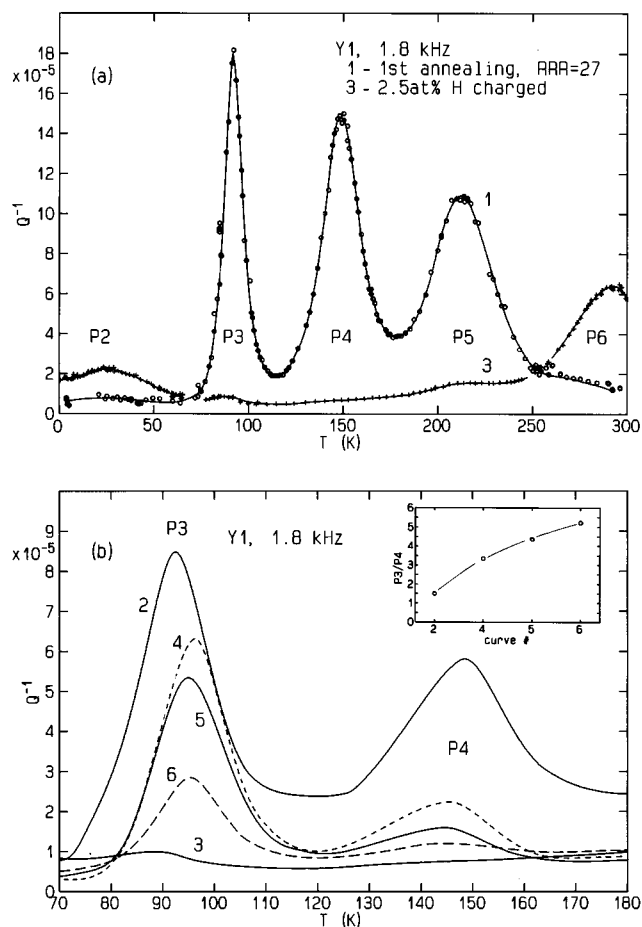


FIG. 4. Influence of H and O charges on the anelastic relaxation spectrum of Y1. The numbering indicates the chronological sequence of the runs. (a) Curve 1, measurement after the first annealing; curve 3, after 2.5 at. % H charge. (b) Curve 2, measurement after the third annealing; curve 4, simultaneous H outgassing and 0.5 at. % O charge at 600 °C; curve 5, 0.2 at. % H charge; curve 6, additional 0.2 at. % H charge. All measurements were carried out on cooling, except curve 1. The inset shows the ratio of the intensity of $P3$ to that of $P4$ for the various curves.

Figure 4(b) also shows that, contrary to what expected, also the increase of the O content decreases peaks $P3$ and $P4$. This can be explained by noting that the O concentration is in the range of the maximum solubility already in the as-received state (540 at ppm). The solubility limit of O in Y has been evaluated at high temperature,²⁸ and the concentration of O in a solid solution below room temperature can be extrapolated from the solvus line down to the temperature at which O is still mobile. As discussed later in Sec. III C, this temperature should be around 400 K, where one obtains $c_O = 300$ at ppm. Therefore, the addition of 0.5 at. % O between runs 2 and 4 does not increase the amount of O in the solid solution, but only that of the precipitated phase. Apparently, the O precipitates do not provide sites for H hopping, and the intensities of $P3$ and $P4$ do not increase. The further decrease of the peaks after adding H is due to saturation of the sites around O, with a consequent blocking effect.

The inset of Fig. 4(b) shows that the ratio of the intensity of $P3$ to that of $P4$ changes with the status of the sample, indicating that the H blocking is more effective for $P4$ than

for $P3$. Instead, the peak shapes and temperatures remain substantially unaffected.²⁹ This fact seems to exclude that $P3$ and $P4$ arise from different types of H jumps within a same O-H complex, because in this case the ratio of the intensities should be constant. Rather, the two processes could be associated to different types of $nO-mH$ complexes, like O-H and O-2H or O-H and 2O-H. In the first case, $P4$ would be caused by the complex pair and $P3$ by the O-2H complex. Curves 4–6 of Fig. 4(b) would be at H contents so high that all the available O atoms have already trapped at least one H atom; the addition of H converts the O-H pairs into O-2H complexes, which start being blocked. In the hypothesis of O-H and 2O-H complexes, both types of clusters are progressively saturated and the complex giving rise to $P4$ is a more effective trap than that giving rise to $P3$.

A peculiarity (not shown here) of the intermediate-temperature spectrum is that the heights of $P4$ and $P5$ (and of $P3$ to a lesser extent) are systematically lower on cooling than on heating; instead, thermal cyclings do not affect process $P2$ at all. This fact denotes that relaxations $P4$ and $P5$ are measured in conditions of nonequilibrium; indeed, both peaks occur in the temperature range where resistivity measurements¹ indicated a transition (~ 180 K) between mobile and immobile H in the time scale of the usual experiments. The characteristic time for the attainment of the equilibrium among O-H complexes, H pairs, and free H can be identified with the relaxation time for H pair formation or dissociation and long-range diffusion, which is $\tau = 10^{-13} \exp(0.6 \text{ eV/kT})$ s; at 180 K, τ is of the order of 1 h.

B. Fast motion of hydrogen

Besides hopping with activation energies between 0.15 and 0.6 eV, hydrogen is observed to perform much faster motion, implying tunneling between neighboring sites. The shortest distance between sites in the hcp lattice is that between pairs of adjacent T sites along the c direction. Such pairs can be occupied by no more than one H atom, which delocalizes itself over both sites. Although this is the only probable geometry for H tunneling, the H fast motion is observed to occur over two or possibly three different times scales. The transition rates deduced from quasielastic neutron spectroscopy (QNS), experiments in ScH_x are of the order of $10^{10} - 10^{12} \text{ s}^{-1}$ between 10 and 200 K;¹⁹ those deduced from NMR in ScH_x (Ref. 13) and from UA experiments in YD_x ,¹⁴ ScH_x and ScD_x (Ref. 15) are in the range $10^7 - 10^{10} \text{ s}^{-1}$ between 10 and 100 K; finally, the rates giving rise to $P2$, as observed in our experiments on YH_x , are in the range $10^3 - 10^6 \text{ s}^{-1}$ between 10 and 60 K.⁷

Although the relaxation rates of $P2$ observed by low-frequency acoustic measurements are considerably lower than those found by ultrasonic, NMR, and QNS experiments, $P2$ is also associated with H tunneling. In fact, if interpreted in terms of a classical overbarrier hopping, it yields unphysically low values for the activation energy and the attempt frequency.

In order to explain how H tunneling between the same type of pairs of adjacent T sites can give rise to so different relaxation rates, different types of tunnel systems can be distinguished: the isolated H atom, the H pair along the c axis, and H near an O atom (possibly a H pair close to O). A

major difference among these types of close pairs of T sites is the asymmetry a between the two site energies and possibly also the tunneling matrix element t . This difference reflects itself in the transition rates, which in the standard two-level system (TLS) model are proportional to $(t/E)^2$, $E = (t^2 + a^2)^{1/2}$ being the energy separation between the levels. Therefore, the larger the asymmetry, the smaller the transition rate, at least until tunneling is coherent. In the case of incoherent tunneling, the situation is more complex, especially when the interaction of the tunneling particle with conduction electrons is relevant. The QNS experiments can detect tunnel systems whose asymmetry is smaller than kT , because otherwise the quasielastic intensity goes to zero. For this reason, the TLS's observed by QNS experiments have been identified with single H atoms in nearly symmetric pairs of sites.¹⁹ Instead, the acoustic experiments are sensitive to TLS's with rates in the range of the vibration frequencies, and the relaxation intensity is proportional to $(a/E)^2$. The slow TLS's detected by NMR and acoustic techniques should be identified with the paired H atoms, which are necessarily asymmetric; the H pairs are certainly abundant in the above-mentioned NMR and UA experiments, since the H/metal ratios are above 0.1. Both NMR and UA have been interpreted in terms of TLS's with a broad distribution of asymmetries and with nearly the same set of coupling parameters to the phonons and conduction electrons.^{14,15}

Due to the lack of data, our anelastic relaxation measurements on YH_x can be compared only with NMR and UA results on YD_x ,¹⁴ ScH_x , and ScD_x ,¹⁵ nonetheless, it appears that we measure still lower relaxation rates and also a different qualitative dependence of the relaxation on the vibration frequency. In our previous study⁷ we have shown that peak $P2$ in $\text{YO}_{0.0027}\text{H}_{0.016}$ exhibits a marked shift to higher temperature with increasing frequency (from 10 to 50 K when f passes from 2.6 to 32 kHz); this indicates that the condition $\omega\tau=1$ for the maximum is roughly satisfied and τ is a rapidly varying function of temperature, presumably due to multiphonon transitions.⁷ On the other hand, the UA peaks show little¹⁴ or no¹⁵ temperature shift, indicating the predominance of slowly varying relaxation rates, i.e., of interaction with the electrons.

The difference may be due to the fact that the pairs of T sites close to O give rise to still different TLS's, responsible for $P2$;⁷ our samples contain much lower H concentrations, and therefore the number of O-H complexes (or of H pairs near O) may be comparable if not predominant over the number of H pairs. Process $P2$ in Figs. 1 and 2 is presumably due to the superpositions of both the relaxations of H pairs and H trapped by O, with the weight of the H pairs increasing with the H content. In order to put clearly in evidence the possible contribution to tunneling from O-H complexes and from H pairs, further measurements are necessary.

C. Motion of interstitial oxygen

The extension of the Q^{-1} measurements up to 550 K reveals a thermally activated process, $P7$, around 450 K in samples Y0, Y2, and Y3. The behavior of $P7$ has been systematically studied in samples Y2 and Y3 and can be described as follows. The process reaches the highest magni-

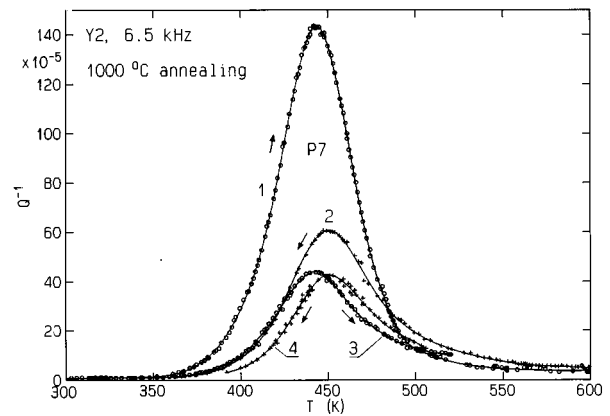


FIG. 5. Elastic energy loss of sample Y2 on heating above room temperature: curve 1 represents the first measurement after the 1000 °C annealing followed by rapid cooling; curves 2, 3, and 4 refer to the subsequent heating-cooling runs.

tude only in the first heating run after the UHV annealing at 1000 °C, followed by cooling to room temperature in less than 10 min (Fig. 5, curve 1). On subsequent cycling between 300 and 600 K, the peak height is progressively reduced (more than 50%) down to nearly stable values (curves 3 and 4). The highest magnitude can be restored by repeating the annealing at 1000 °C followed by rapid cooling. The peak height can also be partially restored if, after heating up to 600 K (Fig. 6, curve 1), the sample is cooled at 5 K/min (curve 2); aging for 1.5 h at the peak temperature reduces the peak height down to a nearly stable value.

A surprisingly good theoretical fit of the stabilized relaxation curves of samples Y2 and Y3 can be achieved in terms of a single-time Debye process, assuming the asymmetry parameter $\Delta E=0$ [Eq. (2), Table I]. This fact and the value of the attempt frequency, which is typical of point defects, suggest that process $P7$ is caused by stress-induced redistribution of interstitial oxygen. The solubility limit of oxygen in yttrium is about 540 at ppm at the peak temperature (550 K), as extrapolated from the data in Ref. 28, and is slightly lower than the O content of our samples. Consequently, the instability of $P7$ with thermal cycling around or aging at the

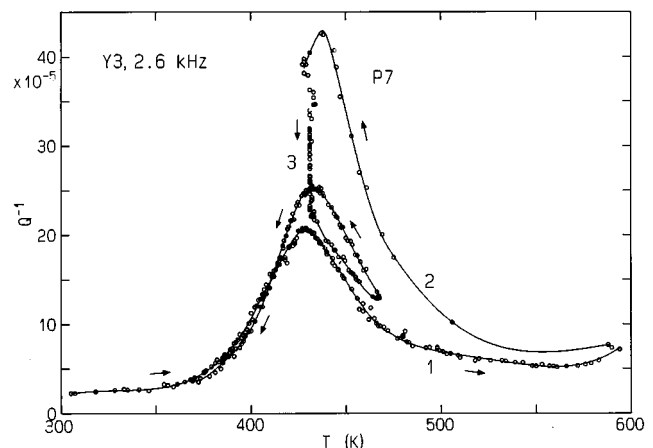


FIG. 6. Effect of the thermal cyclings and aging at the peak temperature on process $P7$ in sample Y3. The measurement of curve 2 was carried out on cooling at 5 K/min.

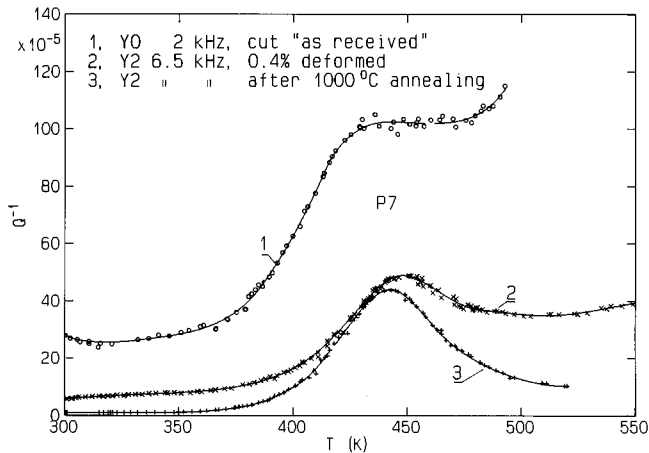


FIG. 7. Elastic energy loss of sample Y0 on heating and cooling (curve 1) and sample Y2 after the thermal cycles of Fig. 5 and subsequent 0.4% plastic deformation (curve 2). Curve 3, reported for comparison, is curve 3 of Fig. 5.

maximum temperature could find its explanation in the O precipitation. Support of this interpretation is given by the observation that in sample Y0, having a lower O content (RRR=34 instead of 27 for Y2), the relaxation curves around *P7* could be retraced during the various cooling and heating measurements (Fig. 7, curve 1), likely because O precipitation did not occur.

The attribution of *P7* to point-defect relaxation is also corroborated by the observation that 0.4% plastic deformation of sample Y2 does not affect the height of *P7* (Fig. 7). The background appearing after deformation above the peak temperature is the signature of a new, unresolved peak (curves 1 and 2), possibly the Snoek-Koester relaxation resulting from dislocations dragging interstitial oxygen.^{26,27}

Considering that in a hcp crystal octahedral and tetrahedral sites remain equivalent after application of any type of stress, hopping of isolated O atoms among sites of the same

type (O Snoek effect) cannot be invoked to explain process *P7*. Therefore, two possible mechanisms are proposed: the stress-induced redistribution of O between the octahedral and tetrahedral sites which are nonequivalent³⁰ or the formation and dissolution of O-O pairs, similar to what proposed for the H pairs giving rise to *P6*. Further investigation is needed to clarify the mechanism.

IV. CONCLUSIONS

We have investigated the nature of the six thermally activated processes appearing in the relaxation spectrum of annealed polycrystalline yttrium in the temperature range of 1–600 K by anelastic relaxation.

The four peaks below room temperature are associated with the H motion. The process at liquid helium temperature is due to H tunneling between asymmetric nearest-neighbor *T* sites. The two processes between 80 and 180 K, fairly described by a single Debye curve, denote a classical over barrier motion of H between trap sites around interstitial O; these peaks are generally not observed, since they disappear at high H content, due to blocking effects. The third process around 200 K, characterized by a broad relaxation curve, has been ascribed to dislocation relaxation dragging interstitial hydrogen.

Above room temperature an intense relaxation peak appears whose height depends on the thermal cyclings (above 400 K). The peak, describable by a single Debye process, has been interpreted as the hopping of interstitial oxygen in a solid solution. In plastically deformed Y, the tail of an additional peak at higher temperature appears, which may be similar to the Snoek-Koester relaxation of bcc metals.

ACKNOWLEDGMENT

The authors wish to thank Dr. I. S. Anderson for supplying the Y samples.

¹P. Vajda, in *Hydrogen in Rare-Earth Metals, Including RH_{2+x} Phases*, Handbook on the Physics and Chemistry of Rare Earths, Vol. 20, edited by K. A. Gschneidner, Jr. and L. Eyring (Elsevier, New York, 1995).

²J. N. Huiberts, R. Griessen, J. H. Rector, R. J. Wijngaarden, J. P. Dekker, D. G. de Groot, and N. J. Koeman, *Nature* **380**, 231 (1996).

³P. Vajda, J. N. Daou, and P. Moser, *J. Phys. (Paris)* **44**, 543 (1983).

⁴J. Voelkl, H. Wipf, B. J. Beaudry, and K. A. Gschneider, Jr., *Phys. Status Solidi B* **144**, 315 (1987).

⁵P. Vajda, J. N. Daou, P. Moser, and P. Remy, *J. Phys. Condens. Matter* **2**, 3886 (1990).

⁶P. Vajda, J. N. Daou, P. Moser, and P. Remy, *Solid State Commun.* **79**, 383 (1991).

⁷G. Cannelli, R. Cantelli, F. Cordero, F. Trequatrini, I. S. Anderson, and J. J. Rush, *Phys. Rev. Lett.* **67**, 2682 (1991).

⁸B. Kappesser, H. Wipf, R. G. Barnes, and B. J. Beaudry, *J. Alloys Comp.* **211**, 249 (1994).

⁹P. Vajda, *Solid State Commun.* **92**, 825 (1994).

¹⁰R. G. Barnes, D. R. Torgeson, T. J. M. Bastow, G. W. West, E. F. W. Seymour, and M. E. Smith, *Z. Phys. Chem. NF* **164**, 867 (1989).

¹¹B. Kappesser, H. Wipf, R. G. Barnes, and B. J. Beaudry, *J. Alloys Comp.* (to be published).

¹²L. R. Lichty, J.-W. Han, R. Ibanez-Meier, D. R. Torgeson, R. G. Barnes, E. F. W. Seymour, and C. A. Sholl, *Phys. Rev. B* **39**, 2012 (1989).

¹³I. Svare, D. R. Torgeson, and F. Borsa, *Phys. Rev. B* **43**, 7448 (1991).

¹⁴R. G. Leisure, R. B. Schwarz, A. Migliori, D. R. Torgeson, I. Svare, and I. S. Anderson, *Phys. Rev. B* **48**, 887 (1993).

¹⁵R. G. Leisure, R. B. Schwarz, A. Migliori, D. R. Torgeson, and I. Svare, *Phys. Rev. B* **48**, 893 (1993).

¹⁶C. A. Swenson, *Phys. Rev. B* **53**, 3680 (1996).

¹⁷P. P. Pal-Val, V. D. Natsik, H.-J. Kaufmann, and A. S. Sologubenko, *Mater. Sci. Forum* **119-121**, 117 (1993).

¹⁸N. L. Adolphi, J. J. Balbach, M. S. Conradi, J. T. Markert, R. M. Cotts, and P. Vajda, *Phys. Rev. B* **53**, 15 054 (1996).

- ¹⁹I. S. Anderson, A. Heidemann, J. E. Bonnet, D. K. Ross, S. K. P. Wilson, and M. W. McKergow, *J. Less-Common Met.* **101**, 405 (1984).
- ²⁰I. S. Anderson, D. K. Ross, and J. E. Bonnet, *Z. Phys. Chem. NF* **164**, S923 (1989).
- ²¹I. S. Anderson, N. F. Berk, J. J. Rush, T. J. Udovich, R. G. Barnes, A. Margel, and D. Richter, *Phys. Rev. Lett.* **65**, 1439 (1990).
- ²²L. Lichty, R. J. Schoenberger, D. R. Torgeson, and R. G. Barnes, *J. Less-Common Met.* **129**, 31 (1987).
- ²³R. G. Barnes, J.-W. Han, D. R. Torgeson, D. B. Baker, M. S. Conradi, and R. E. Norberg, *Phys. Rev. B* **51**, 3503 (1995).
- ²⁴A. S. Nowick and B. S. Berry, *Anelastic Relaxation in Crystalline Solids* (Academic, London, 1972).
- ²⁵M. H. Youssef and P. G. Bordoni, *Philos. Mag. A* **67**, 883 (1993).
- ²⁶A. Seeger, *Phys. Status Solidi A* **55**, 457 (1979); A. Seeger, M. Weller, J. Diehl, Z. Zau, J. Zhang, and T. S. Kê, *Z. Metallkd.* **73**, 1 (1982).
- ²⁷M. Weller, *J. Phys. (Paris) Colloq.* **44**, C9-63 (1983).
- ²⁸E. Fromm and E. Gebhardt, *Gase und Kohlenstoff in Metallen* (Springer, Berlin, 1976), pp. 364–368. The O solubility limit is reported to be $\log_{10}(c_{\text{O}}/\text{at. \%})=2.17-1480/(T/\text{K})$ between 600 and 1200 °C.
- ²⁹A small temperature shift of *P3* is observed after addition of 0.5 at. % O. Similar effects have been reported for the relaxation of the O-H pair in Nb [G. Cannelli, R. Cantelli, F. Cordero, and F. Trequatrini, *Mater. Sci. Forum* **119-121**, 29 (1993)] and temperature shifts up to 50 K have been observed in dilute substitutional alloys $\text{Nb}_{1-x}\text{Ti}_x\text{H}_y$ [G. Cannelli, R. Cantelli, and M. Koiwa, *Philos. Mag. A* **46**, 483 (1982)]. These effects have been interpreted in terms of elastic interaction among the defect complexes [G. Cannelli, R. Cantelli, and F. Cordero, *Phys. Rev. B* **32**, 3753 (1985)].
- ³⁰F. Povo and E. A. Bisogni, *Acta Metall.* **15**, 701 (1967).